Research Square

Preprints are preliminary reports that have not undergone peer review.
They should not be considered conclusive, used to inform clinical practice,
or referenced by the media as validated information.

Eggshell-Derived CaO@g-C_3N_4 Catalyst: An Efficient, Reusable and Economical Approach for the Synthesis of Pyrano[2,3-d]Pyrimidine Scaffolds as Potent Anticancer Agents with Molecular Docking Study

Sachin Khade[1]
Sanjay Ghodawat University
Deepak Mahuli
Bharati Vidyapeeth College of Pharmacy
Prafulla Choudhari
Bharati Vidyapeeth College of Pharmacy
Pallavi Bhange[1]
pallavi.ncl@gmail.com

Sanjay Ghodawat University

Research Article

Keywords: Calcium oxide, pyrano[2,3-d]pyrimidine, green synthesis, Anticancer agent

Posted Date: May 21st, 2026

DOI: https://doi.org/10.21203/rs.3.rs-9516313/v1

License: This work is licensed under a Creative Commons Attribution 4.0 International License.
Read Full License

Additional Declarations: No competing interests reported.

Eggshell-Derived CaO@g-C_3N_4 Catalyst: An Efficient, Reusable and Economical Approach for the Synthesis of Pyrano[2,3-d]Pyrimidine Scaffolds as Potent Anticancer Agents with Molecular Docking Study

Sachin Khade[1], Deepak Mahuli[2], Prafulla Choudhari[3], and Pallavi Bhange[1]*

[1]School of Chemical Sciences, Sanjay Ghodawat University, Atigre, Kolhapur-416118, India.

[2]Department of Pharmacology, Bharati Vidyapeeth College of Pharmacy, Kolhapur 416 013 Maharashtra, India

[3]Department of Pharmaceutical Chemistry, Bharati Vidyapeeth College of Pharmacy, Kolhapur 416 013 Maharashtra, India

Abstract:

We describe a very efficient and environmentally friendly method for the synthesis of pyrano [2,3-d] pyrimidine derivatives using the CaO catalyst prepared from waste eggshell and the CaO@g-C_3N_4 catalyst. Various physicochemical analyses, such as XRD, SEM, and EDX analysis of the CaO@g-C_3N_4 sample, verify that CaO was successfully incorporated into the g-C_3N_4 matrix. This green method is performed under mild conditions, producing high yields (85-96%) without the use of toxic chemicals and harsh solvents, making it a green and very cheap method compared to the existing ones. This heterogeneous catalyst system performs very well in the presence of green solvents, which enables the production of a large amount of the desired product. The special CaO@gC_3N_4 catalyst system exhibits high catalytic activity, making the desired condensation and cyclization reaction that led to the formation of the pyrano [2,3-d] pyrimidine ring system possible. The products were characterized by ^1H, ^{13}C NMR, and mass spectrometry. This method not only valorizes waste but also provides a green approach for the design of a strong, reusable, and environmentally friendly method for the preparation of heterocycles that are of great importance in medicinal chemistry, with great potential in the design of new bioactive molecules. The synthesized Pyrano [2,3-d] pyrimidine derivatives are tested for in vitro anticancer activity as well as their molecular docking studies against SH-SY5Y cells. Molecular docking of the synthesised derivatives (4a-c) performed against human anaplastic lymphoma kinase (ALK) indicates good binding affinity.

Keywords: Calcium oxide, pyrano[2,3-d]pyrimidine, green synthesis, Anticancer agent.

*Corresponding author: Dr. P. D. Bhange, Email: pallavi.ncl@gmail.com, pallavi.bhange@ch.sguk.ac.in

Sachin Khade[1]; **Email:** khadesachin2@gmail.com

Deepak Mahuli[2]; **Email:** deepak.mahuli@bharatividyapeeth.edu

Prafulla Choudhari[3]; **Email:** prafulla.choudhari@bharatividyapeeth.edu

1. Introduction:

The shift toward circular and sustainable chemical technologies has intensified interest in converting biogenic waste into functional catalytic materials. Eggshell waste, produced in significant volumes globally, is an exceptionally appealing feedstock owing to its elevated $CaCO_3$ concentration and the simplicity of its conversion into catalytically active CaO or CaO-rich phases [1-3]. Thermal activation, nanostructuring, and surface modification of CaO from eggshells have repeatedly shown that it has a strong basicity, is very stable, and can be used in a wide range of organic transformations, biodiesel production, and esterification [4, 5]. There is a pressing need for environmentally responsible strategies to manage and repurpose eggshell waste [6]. Through straightforward calcination, these eggshells can be converted into calcium oxide (CaO), a versatile, renewable material with significant potential as a green catalyst [7]. These features position eggshell-based catalysts as promising alternatives to conventional bases in the synthesis of heterocyclic frameworks.

Pyrano[2,3-d]pyrimidines are a significant category of fused O, N-heterocycles exhibiting various pharmacological properties, such as antimicrobial [8], antitubercular [9], antitumor [10], anti-inflammatory [11], antifungal [12], anticancer [13] and EGFR/HER2 Inhibitory effects [14] as mentioned in Figure 1. Their modular assembly via multicomponent reactions (MCRs) adheres to green chemistry principles, providing high atom economy, brief synthetic pathways and operational ease [15].

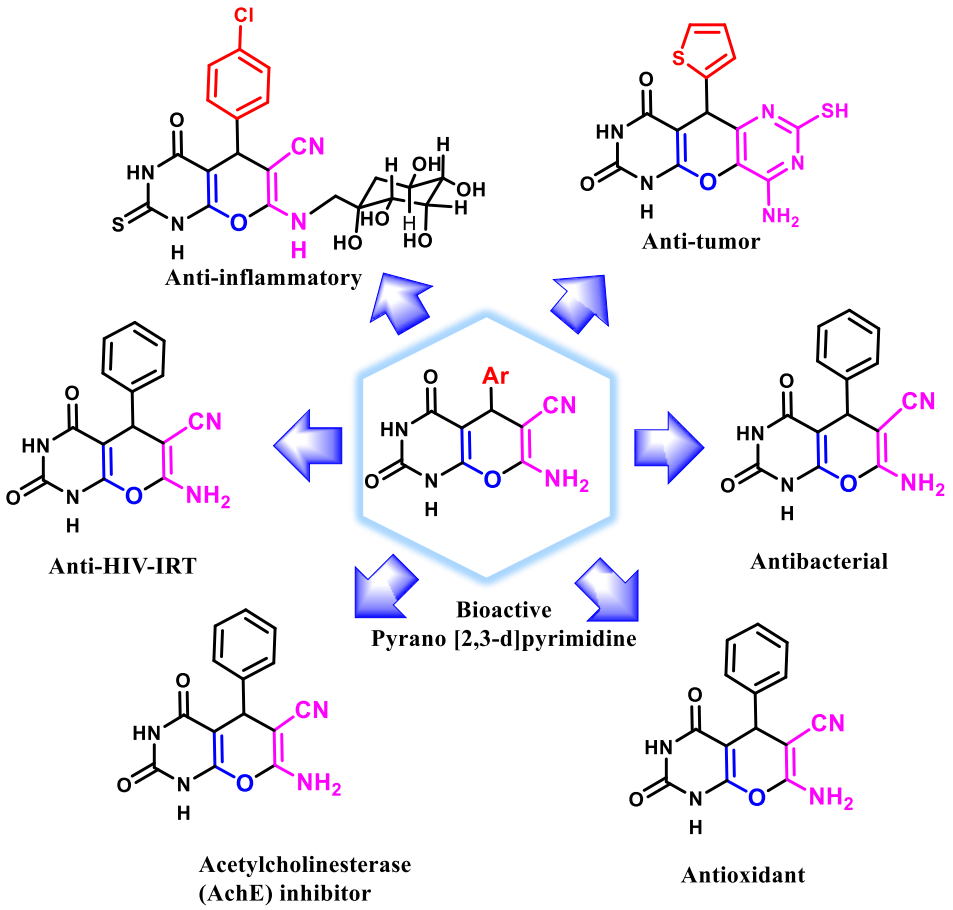


Fig. 1. Biologically important Pyrano[2,3-d]pyrimidines drugs.

A number of catalytic systems have been developed for the facilitation of MCRs reactions, including traditional catalysts like trifluoroacetic acid [16], boric acid ($B(OH)_3$) [17], K_2O/Al_2O_3-CaO [18], and Fe_3O_4,Ag@starch [19]. Amino acid-based complexes (Zn[(L)-Proline]$_2$) [20], cetyltrimethylammonium bromide (CTAB) [21], dibutyl amine (DBA) [22], sulfonic acid nanoporous silica (SBA-Pr-SO_3H) [23], as well as ionic liquids and wide range of metal-oxide nanocatalysts that can provide rapid reactions and high yields under mild or green conditions [24]. Moreover, recent studies have highlighted the effectiveness of cooperative and hybrid catalytic systems, such as ionic-liquid-functionalized magnetic nanoparticles and metal-organic framework derivatives, which provide improved catalytic activity and recyclability [25-29].

However, many of the catalysts reported to date are associated with a number of limitations, including toxicity, high cost, long reaction times, poor recyclability, catalyst degradation, and metal leaching. The catalytic activity of many of these systems is also reduced after multiple uses due to exposure to harsh reaction conditions and strong interactions with substrates. Thus, the development of advanced catalytic systems with improved stability, longevity, and environmental compatibility is a major challenge, especially for large-scale applications. Despite these advances, the application of waste catalysts, particularly eggshell-derived CaO, in the synthesis of pyrano[2,3-d]pyrimidines remains poorly explored. With their low cost, basicity, negligible environmental impact, and high reusability, eggshell-derived catalysts provide a highly attractive avenue for merging green catalyst design with efficient multicomponent heterocycle synthesis. The current study continues along this new avenue with the goal of promoting sustainable methods for the assembly of biologically valuable pyrano[2,3-d]pyrimidine cores *via* environmentally responsible catalysis.

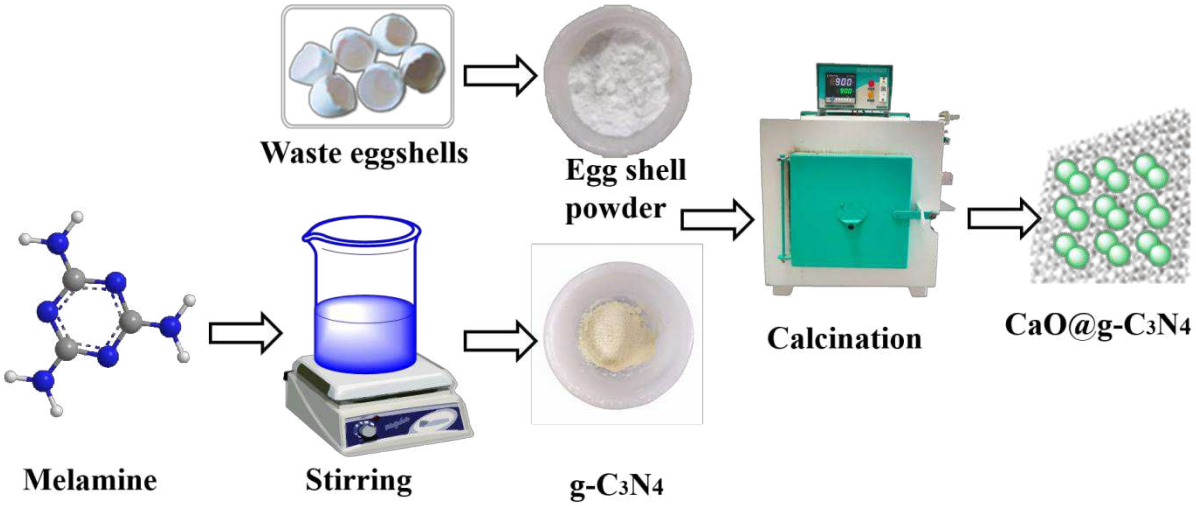
2.0 EXPERIMENTAL:

2.1 Preparation of Catalyst:

The eggshell waste obtained from the household waste was collected, cleaned, and first washed thoroughly with water to remove the membrane and impurities that are adhered to the surface of the eggshells and then dried at 110°C for 2 h. The dried sample was crushed into a fine powder. The eggshell powder was then calcined at a temperature of 950°C in a muffle furnace for 3 h (ramp 5°C/min) under air to give CaO. The white powder was then cooled to room temperature and stored in a desiccator. The above process converts the calcium carbonate present in the eggshells to calcium oxide (CaO), which is the active component of the catalyst [30].

2.2 Preparation of CaO@g-C_3N_4 Catalyst:

In a general method, 1 gm of melamine was dissolved in 20 ml of isopropyl alcohol and stirred for 2h using a magnetic stirrer. Then, 0.1 gm of CaO was added to the above solution and stirred for 3 hours with the addition of 40 ml of distilled water. The resulting solution was filtered and dried at 100°C for 1 h and then the mixture was finally calcined at 500°C for 2h in a muffle furnace. The schematic diagram is represented in Scheme 1.



Scheme 1. Schematic representation of preparation of CaO@g-C_3N_4 catalyst

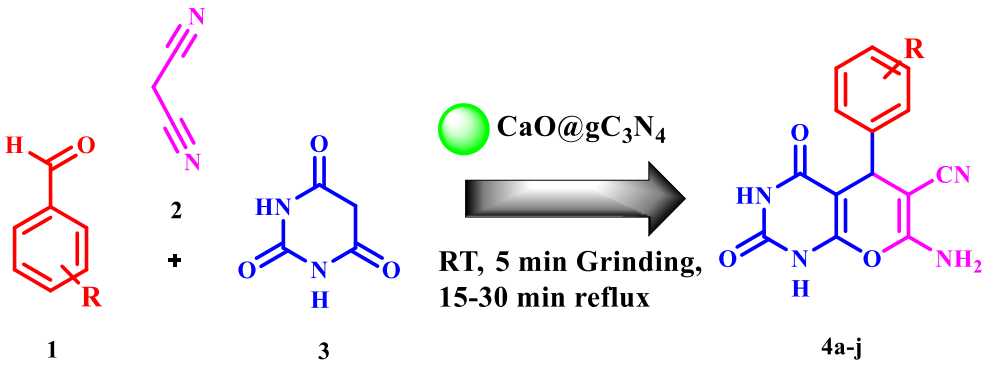
2.3. Characterization studies

The crystallographic phase and purity of the synthesized sample were analyzed by XRD at room temperature using a Rigaku-manufactured Ultima IV diffractometer with Cu Kα1 radiation (λ = 1.5406 Å). The diffractometer was calibrated with a Si disc prior to the collection of XRD data. Powder XRD data was collected for the sample over the 2θ range of 05-90° with a step size of 0.02°. The scanning electron microscope JOEL JSM-6360 was applied for the analysis of the surface morphology. The elemental composition of the as-prepared CaO was analyzed by energy-dispersive X-ray spectra (EDX) on the JASCO spectrofluorometer. Fourier-transform infrared spectrophotometer (FTIR) Spectra was recorded on a PerkinElmer spectrophotometer. The ^{1}H and ^{13}C NMR spectra were recorded on a 400 MHz Varian spectrometer in DMSO-d_6 solvent, with tetramethylsilane (TMS) as an internal standard. Chemical shifts (ı) are expressed in ppm, while coupling constants are in Hz. Mass spectra were recorded on a (WATER) Spectrometer with PDA and SQ detector (mobile phase: 0.05% formic acid in water, software: Mass Lynx, ionization mode: ES+/ES-, capillary voltage: 1.50 kV). The melting points were measured using an electrothermal melting point apparatus in capillary tubes, which was not corrected.

2.4. General Procedure for the Synthesis of Pyrano[2,3-d]pyrimidine derivatives

As shown in Scheme 2, combination of aromatic aldehydes (1, 2.0 mmol), malononitrile (2, 2.1 mmol, 66 mg), and barbituric acid (3, 1.0 mmol, 128 mg) was well ground with eggshell-derived CaO@C_3N_4 catalyst (100 mg) in a mortar and pestle for 5 minutes under solvent-free conditions at room temperature. The reaction mixture was then transferred to a 25 mL round-bottom flask and 5 mL of ethanol was added to it as a solvent. The obtained suspension was refluxed at 60ºC for 15 to 30 minutes. The progress of the reaction was checked by TLC using hexane/ethyl acetate (3:2) as the eluent. After completion, the reaction mixture was dissolved in hot ethanol and filtered to remove the catalyst. The evaporation of solvent in vacuo yielded crude residue, which was recrystallized from hot ethanol to obtain the pyrano[2,3-d]pyrimidine derivatives (4a–h) as crystalline solids in excellent yield. The catalyst was thoroughly washed with ethanol to remove any adsorbed organic residues and then heated at 120°C for 1 hour to regenerate its activity. The CaO and CaO@gC_3N_4 composites act as a

heterogeneous catalyst, and their recovery and reuse were tested to check the stability and efficiency of the catalyst over multiple cycles.



Scheme 2. Reaction with Functionalized Catalyst

2.5. MTT ASSAY: Experimental procedure

SH-SY5Y cells were incubated at a concentration of 1 × 10^4 cells/ml in culture medium for 24 h at 37°C and 5% CO_2. Cells were seeded at a concentration (100µl) 10^4cells/well) in 100µl culture medium and 20, 40, 60, 80, and 100 µg/ml of samples into microplates (tissue culture grade and 96 wells), respectively. Control wells were incubated with DMSO (0.2% in PBS) and the cell line [31]. All samples were incubated in triplicate. Controls were maintained to determine the control cell survival and the percentage of live cells after culture. Cell cultures were incubated for 24 h at 37°C and 5% CO_2 in a CO_2 incubator. After incubation, the medium was completely removed, and 20 µl of MTT reagent (5 mg/ml PBS) was added. After the addition of MTT, cells were incubated for 4h at 37°C in a CO_2 incubator. The formazan crystal formation observed under a microscope. The yellowish MTT was reduced to dark-colored formazan by viable cells only. After incubation 200 µl of DMSO was added to dissolve the formazan crystals (kept for 10 min) and incubated at 37°C (wrapped with aluminum foil). Triplicate samples were analysed by measuring the absorbance of each sample by a microplate reader at a wavelength of 550 nm.

Molecular Docking:

Molecular docking analysis of the synthesised pyrano[2,3-d] pyrimidine derivatives was carried out to identify the possible mode of the actions for the anticancer potential. X-ray crystal structure of human anaplastic lymphoma kinase in complex with CH5424802 (PDB ID: 3AOX) was utilised as protein target which was downloaded from free protein databank www.rcsb.org. Docking analysis was performed using autodock vina in chimera 1.19. Analysis of the docking results was performed using academic version of Maestro 14.5. [32-35].

3. Result and discussion

3.1. XRD: Characterization

The X-ray diffraction (XRD) pattern of the CaO derived from the waste eggshells indicates strong diffraction peaks, indicating a highly crystalline nature after calcination at 950°C, as depicted in Figure 2. The diffraction peaks match well with the standard face centred cubic structure of CaO (JCPDS No. 77-2376) [36]. The (111), (200), (220), (311), and (222) crystal planes of cubic CaO correspond to the characteristic diffraction

peaks that appear at 2θ values of 32.20°, 37.34°, 53.85°, 64.15°, and 67.37°. The intensity and sharpness of the diffraction peaks indicate that $CaCO_3$ has been successfully converted into high-temperature crystalline CaO. The addition of CaO to graphitic carbon nitride (g-C_3N_4) introduces a new diffraction peak at 2θ ≈ 26.50°. This diffraction peak corresponds to the (002) interlayer stacking plane of g-C_3N_4, indicating the formation of the graphitic structure. The appearance of both CaO and g-C_3N_4 diffraction peaks indicates that CaO has been successfully incorporated into the g-C_3N_4 support without altering the crystal structure of either component. The average crystallite size of the CaO component was using the Scherrer equation; we found that the average crystallite size of the CaO phase was 17 nm [37].

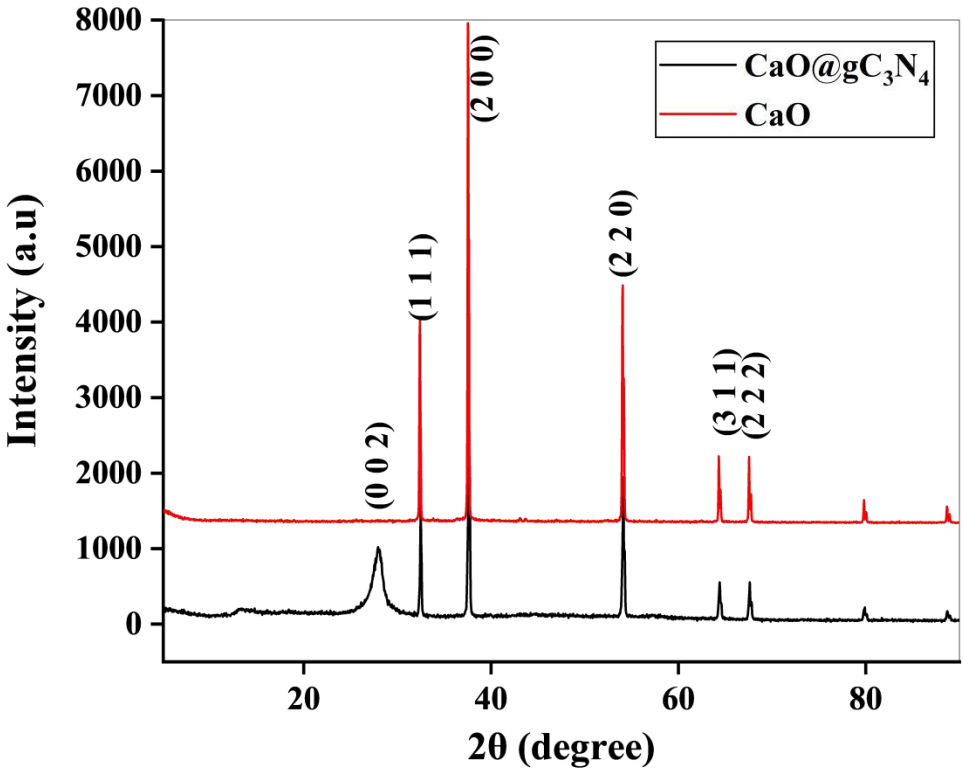


Fig. 2. The powder XRD patterns of the CaO and CaO@g-C_3N_4 composite.

3.2. SEM, EDX, and FTIR Analysis of the Catalyst

Scanning Electron Microscopy (SEM) is used to look at the size and shape of the CaO particles made from waste eggshells. The examination of calcium oxide (CaO) indicates a consistent particle size distribution, with dimensions varying from 5 to 10 µm, as illustrated in Figure 3. The FESEM image demonstrate that the small, irregularly shaped particles are formed. The particles' edges look to be welded together because of the extreme temperature. Supplementary information shows the EDX analysis of calcium oxide and the CaO@gC_3N_4 composite. The results show that the sample is very pure CaO and does not contain any other elements or contaminants that are important. The presence of nitrogen and carbon in the CaO@gC_3N_4 composite shows that graphitic carbon nitride (g-C_3N_4) has been added, making it a hybrid material. Figure 4 shows that the FTIR spectrum shows that CaO was successfully loaded onto graphitic carbon nitride. The broad peak indicates the existence of surface hydroxyl groups, while the distinct peaks for C=N, C=C, and C≡N validate the

structural integrity of graphitic carbon nitride. The Ca–O vibrations also strongly support the idea that CaO and the carbon nitride material interact with each other [38].

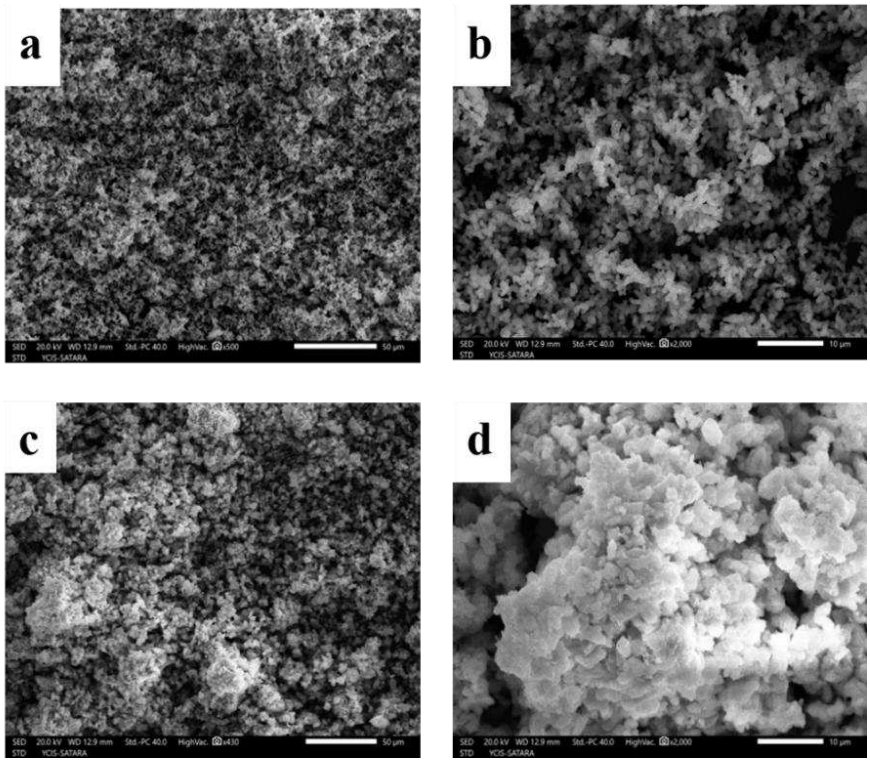


Fig. 3: FESEM image of CaO (a, b) and of CaO@gC_3N_4 composite (c, d**)** respectively.

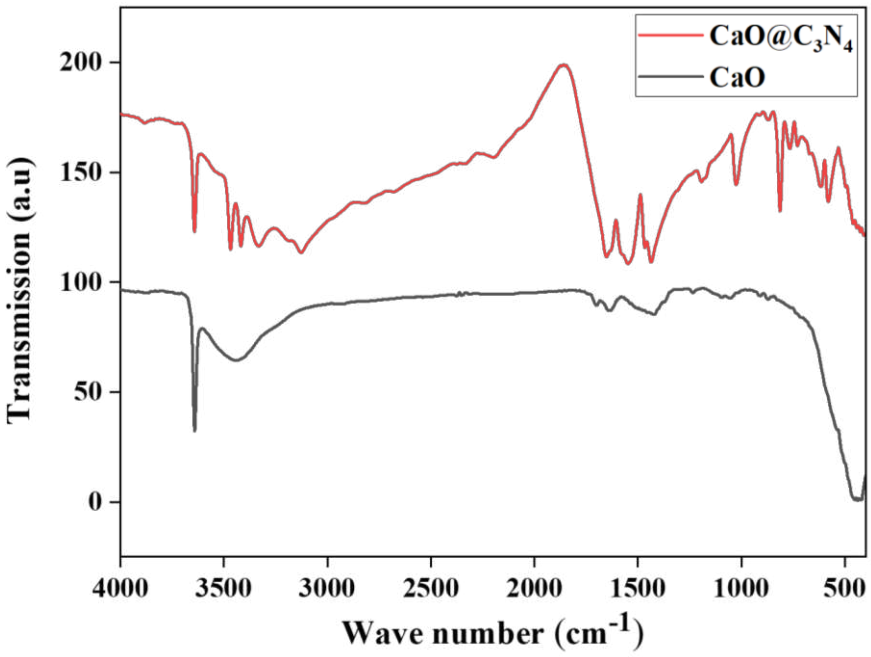
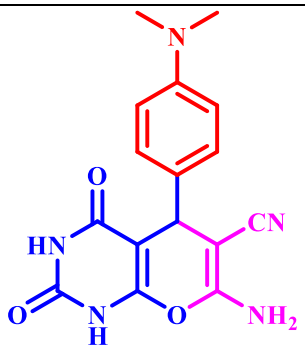
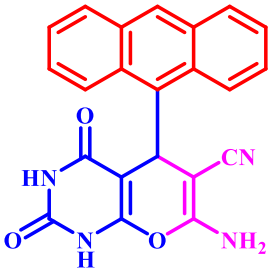
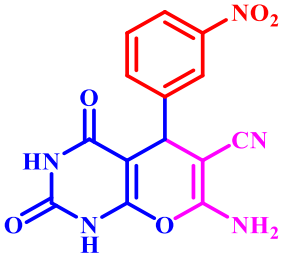
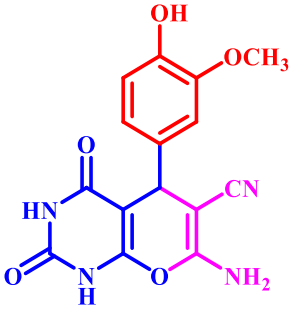


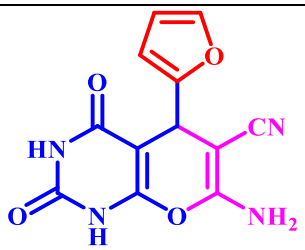
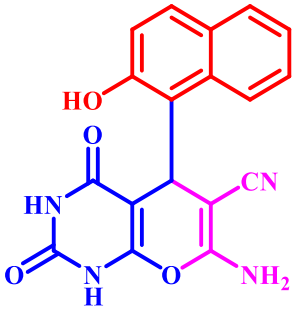
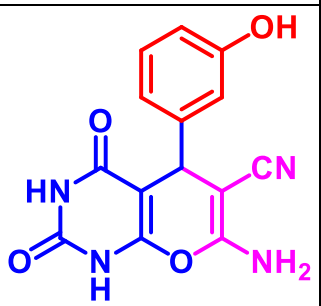
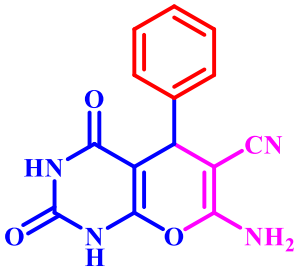
Fig.4. FTIR Spectra of CaO and CaO@g-C_3N_4 composite.

3.3 Synthesis of pyrano[2,3-d]pyrimidine derivatives

The synthesis of pyrano[2,3-d]pyrimidine derivatives was carried out using CaO@gC$_3$N$_4$ as a catalyst. The efficiency of CaO@gC$_3$N$_4$ in promoting the formation of pyrano[2,3-d]pyrimidine derivatives is shown in Table 1, entries 1-8. The results demonstrate that the proposed approach offers significant advantages over earlier methods, particularly in terms of higher product yield and reduced reaction time.

Table 1. CaO@g-C$_3$N$_4$ catalyzed synthesis of *pyrano[2,3-d]pyrimidine* derivatives.

Comp. No	**Products (4a-h)**	**Color**	**Time, min**	**% Yield**	**M.P °C**		**Ref.**
					Obs.	**Lit.**	
1		Orange	30	87	232	229-231	[27]
2		Red	25	96	283	286	This study
3		white	25	91	273	272-274	[11-17]
4		Yellow	30	85	283	-	This study

5		Pale green	25	85	285-287	-	This study
6		Yellow	30	91	283	280-282	[11-17]
7		white	30	87	165	161-163	[11-17]
8		white	30	90	206	205-206	[11]

3.4 Effect of solvent on the yield of pyrano[2,3-d] pyrimidine derivatives

As shown in Figure 5, the reactions were carried out using non-toxic solvents, such as ethanol and water, with no need for harsh reagents. The ethanol water system provides sufficient polarity to dissolve the reactant and also stabilize the intermediate formed during the reaction and accelerate the rate of reaction. This approach aligns with the principles of green chemistry, emphasizing minimal environmental impact and energy consumption. By minimizing the use of harmful solvents and reagents and enabling catalyst reuse, the methodology reduces its environmental footprint. This makes it a valuable addition to the field of sustainable organic synthesis.

Table 2. Effect of Solvent on synthesis of *pyrano[2,3-d]pyrimidine* derivatives

Entry	Solvent	Temperature	Time (min)	Yield (%)
1	Water	RT (30℃)	25	80
2	Ethanol	RT	15	90
4	**Aq.ethanol(2:1)**	**60℃**	**30**	**96**
5	Methanol	RT	30	92
6	Acetonitrile	RT	30	75
7	DMSO	RT	30	85
8	THF	RT	30	72
9	Isopropyl alcohol	RT	30	78

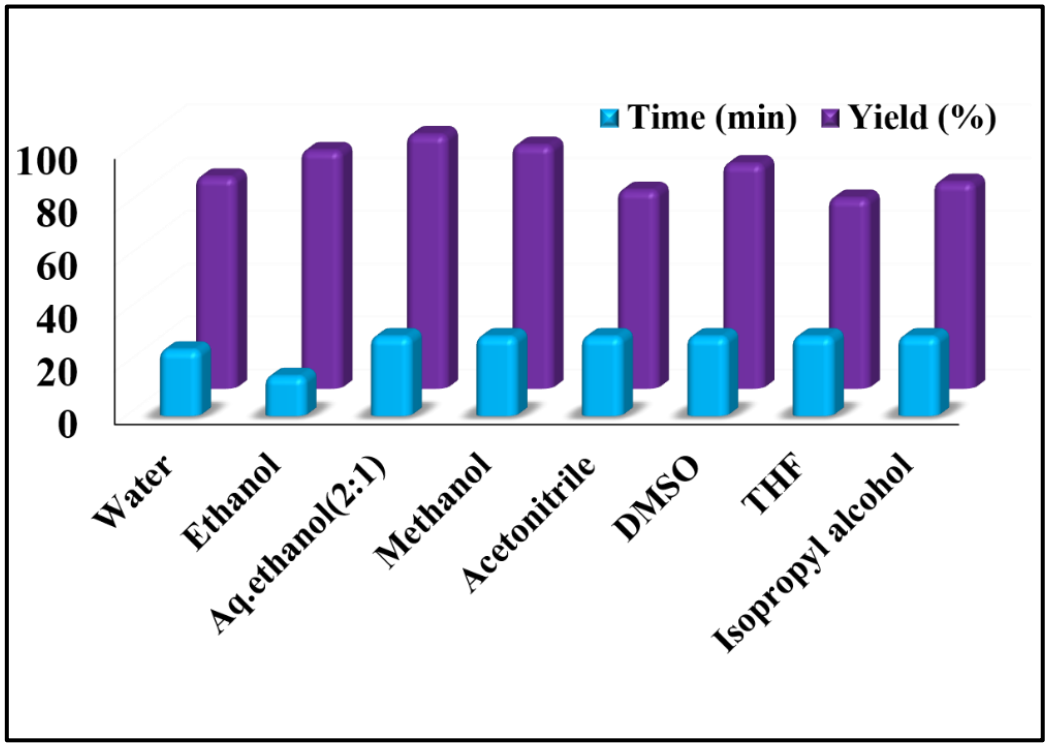


Fig.5. Effect of solvent conditions on yield for the product 4a using $CaO@gC_3N_4$ composite as a catalyst.

3.5 Effect of amount of catalyst on the yield of pyrano[2,3-d] pyrimidine derivatives

The influence of $CaO@gC_3N_4$ catalyst loading on the reaction efficiency was systematically studied by varying the catalyst amount from 0.00 to 0.25 g under solvent-free conditions (Figure 6). The yields of the target compound were found to increase with catalyst loading up to a certain point. These results indicate that the catalytic activity of $CaO@gC_3N_4$ increases significantly up to 0.20 g. The maximum yield of 96% was achieved with 0.20 g of catalyst, suggesting that this is the optimal amount required for efficient conversion under the given conditions. Increasing the catalyst loading beyond this point did not enhance the yield further; instead, it

led to a slight decline or stagnation. This plateau in performance may be attributed to the excessive catalyst causing inhomogeneity in the reaction mixture, which can interfere with effective contact between reactants and the active catalytic sites. Overloading the system likely leads to agglomeration or poor dispersion, reducing the accessibility of the catalyst surface. The reactions were completed with excellent yields (85-95%) in a relatively short period of 2-3 hours. This represents a significant improvement over traditional methods, which often require higher temperatures or longer reaction times.

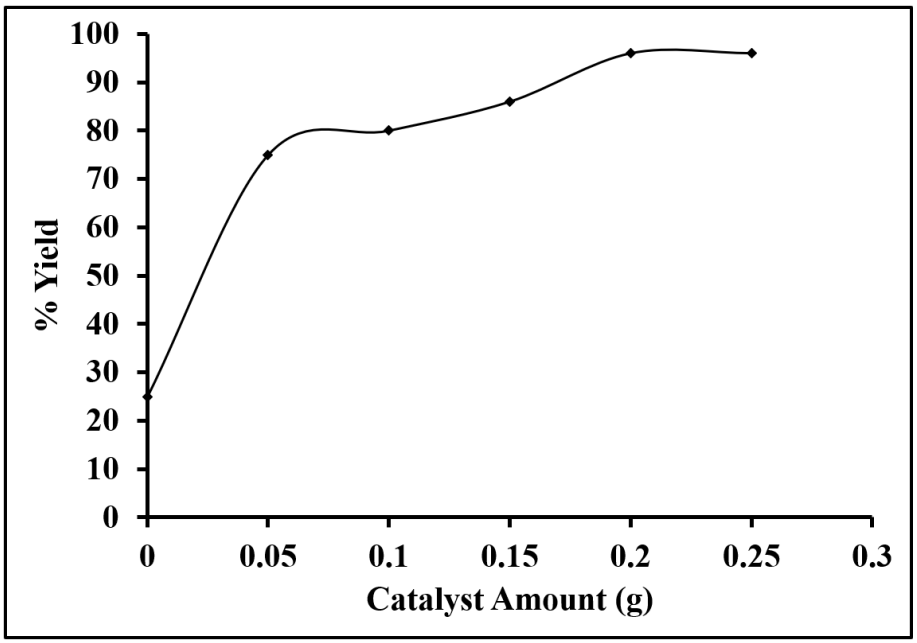


Fig.6. Influence of the amount of catalyst in the synthesis of compound 4a using CaO@gC_3N_4 composite as a catalyst.

3.6 Reaction Mechanism:

Research indicates that the catalyst promotes reactions via dual interactions. The CaO part activates electrophilic substrates by giving them Lewis basic sites, and the g-C_3N_4 part helps electrons move and keeps intermediates stable. Figure 7 shows the suggested way that CaO@g-C_3N_4 can be used to make pyrano[2,3-d]pyrimidine derivatives without using any solvents. At first, the basic O^{2-} sites of CaO, which are held in place by the g-C_3N_4 support, take the acidic proton from malononitrile (2) to make a carbanion species that is very nucleophilic. This carbanion reacts with the aromatic aldehyde (3) in a Knoevenagel condensation. At the same time, the carbonyl group of the aromatic aldehyde is activated by Lewis-acidic Ca^{2+} centers on the catalyst surface, creating the arylidene-malononitrile intermediate. Then, the catalyst's basic sites take away a proton from the active methylene group of barbituric acid (1), making an enolate that adds to the electrophilic C=C bond of the intermediate in a Michael addition. The required pyrano[2,3-d] pyrimidine products are made by intramolecular cyclization and then tautomerization [39,40].

The synergistic catalytic effect of CaO@g-C_3N_4 comes from the fact that it has two functions: the surface O^{2-} sites promote deprotonation and proton transfer steps, while the Ca^{2+} and nitrogen-rich g-C_3N_4 matrix stabilize charged intermediates and improve substrate adsorption through π–π and hydrogen-bonding

interactions. This cooperative activation speeds up both condensation and cyclization when the grinding is done in a mild, solvent-free environment.

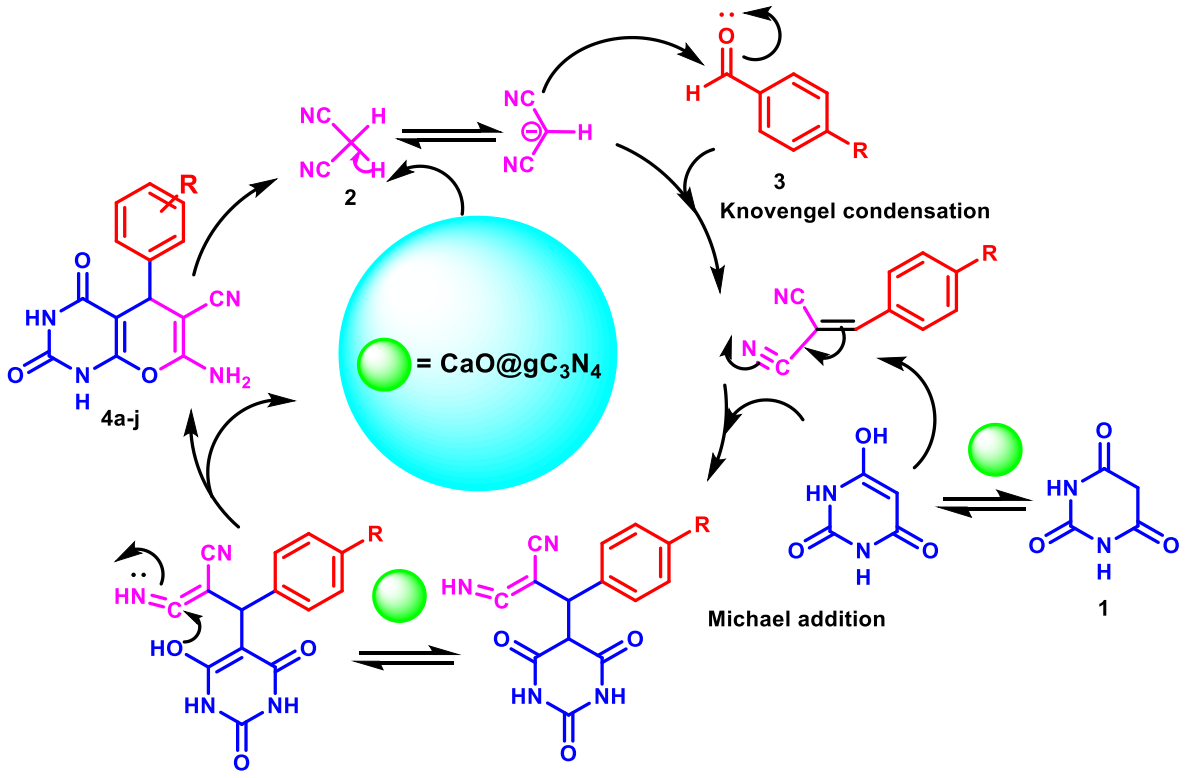


Fig. 7. Plausible mechanistic pathway for synthesis of pyrano[2,3 d] pyrimidine derivatives

3.7 Recyclability of the CaO@gC₃N₄ catalyst:

The regenerated catalyst was subsequently reused under identical reaction conditions for four consecutive cycles. The CaO@gC₃N₄ nanocatalyst retained high catalytic performance throughout the recycling tests, with only a minimal decline in product yield. The dried catalyst was then reused in a fresh reaction with the model substrates, yielding a compound with 80-97% efficiency. This process was repeated two more times, and as shown in Figure 8, the catalyst demonstrated consistent performance, maintaining its activity for up to four cycles with minimal loss in efficiency. The CaO@gC₃N₄ catalyst showed good reusability, maintaining its catalytic activity over five cycles with little to no loss of performance. This feature is essential for improving the sustainability of the process by reducing the need for fresh catalyst material. Overall, these findings demonstrate the potential of the CaO@gC₃N₄ catalyst to offer an efficient, sustainable, and green approach to organic synthesis.

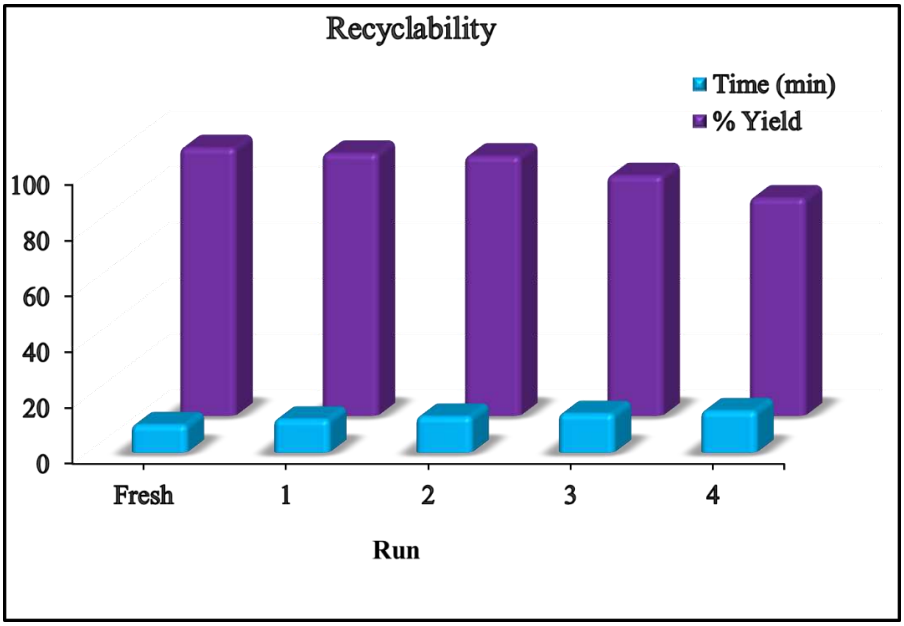


Fig.8. Recyclability of the CaO@gC_3N_4 catalyst for the synthesis of compound 4a.

3.8 The anticancer activity (MTT assay)

The anticancer activity of samples 4a, 4b, and 4c was evaluated against the *SH-SY5Y* neuroblastoma cell line using the MTT assay, and the results are shown in the Figure 9. All samples exhibited a concentration-dependent increase in cytotoxicity, indicating that higher concentrations enhanced cell inhibition. The standard showed the highest percentage of inhibition, reaching nearly 90% at 100 µg/ml as shown in Table 3. Among the test samples, 4a displayed the strongest anticancer activity with approximately 55–60% inhibition at the highest concentration, followed by 4c and 4b, which showed moderate cytotoxic effects as shown in Figure 10. Overall, the results suggest that the test samples, particularly 4a, possess significant anticancer potential against *SH-SY5Y* cells, though their activity remains lower than that of the standard drug [41-45].

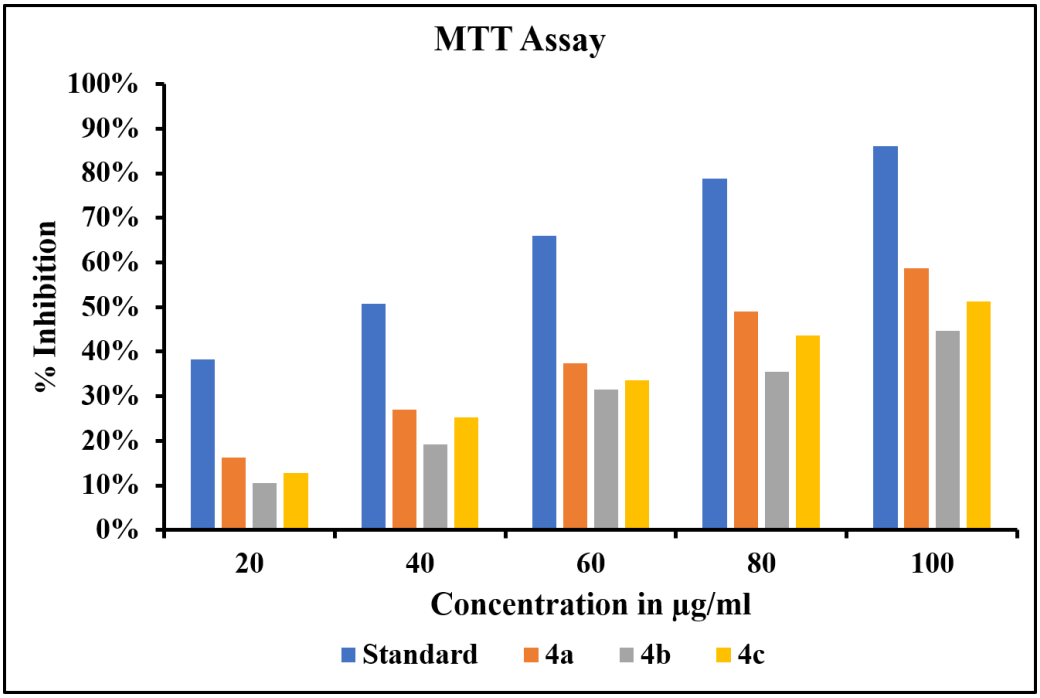


Fig.9. Anticancer evaluation (In vitro study) of compounds 4a to 4c against the SH-SY5Y neuroblastoma cell line

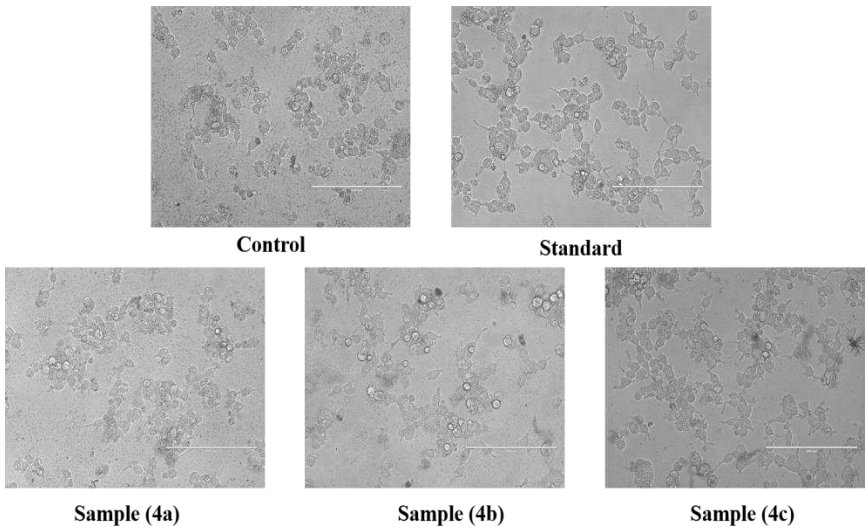


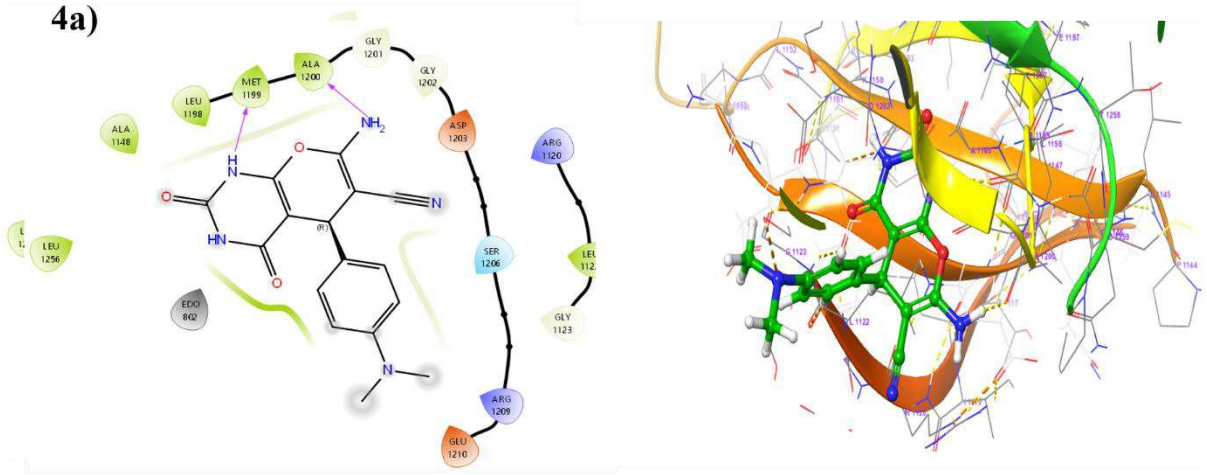
Fig.10. Inverted microscopic images of *SH-SY5Y* neuroblastoma cell line before and after treatment

Table 3- Effects of compounds (4a-c) against SH-SY5Y Cell lines

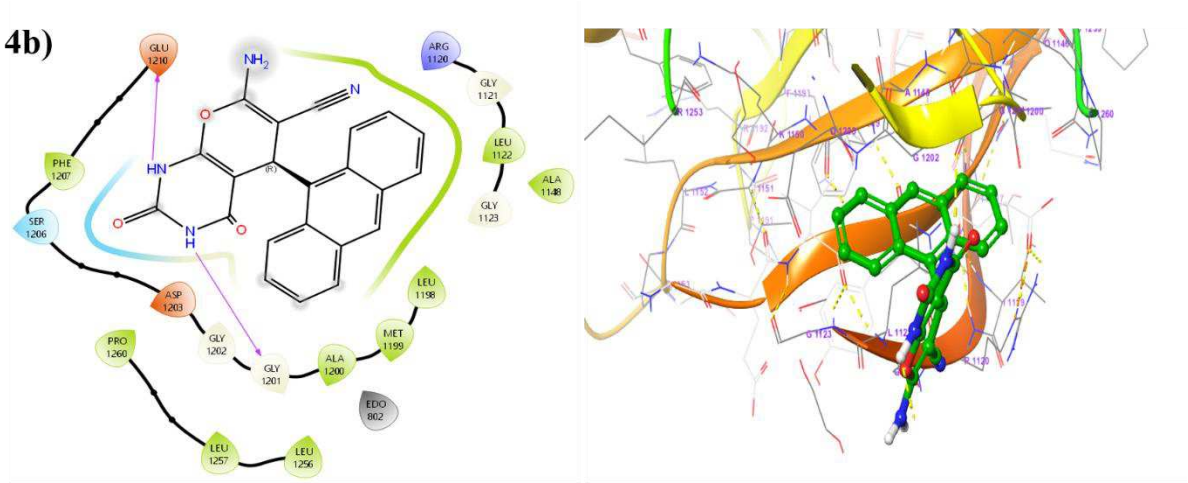
SR NO	SAMPLE CODE	Conc. (µg/ml)	OD			Mean	% Of Inhibition	% Of Viability	IC50 (µg/ml)
1	Control		1.482			-	-	-	-
2	Standard	**20**	0.916	0.915	0.916	**0.915**	**38.25%**	**61.75%**	
	(5,Flurour-acil)	**40**	0.732	0.729	0.734	**0.731**	**50.67%**	**49.33%**	**49.33**
		60	0.507	0.504	0.502	**0.504**	**65.99%**	**34.01%**	
		80	0.315	0.312	0.314	**0.313**	**78.87%**	**21.13%**	
		100	0.208	0.205	0.207	**0.206**	**86.09%**	**13.91%**	
3	4a	**20**	1.243	1.245	1.240	**1.242**	**16.19%**	**83.81%**	
		40	1.080	1.083	1.084	**1.082**	**26.99%**	**73.01%**	
		60	0.927	0.925	0.930	**0.927**	**37.45%**	**62.55%**	**51.36**
		80	0.758	0.754	0.757	**0.756**	**48.99%**	**51.01%**	
		100	0.612	0.613	0.615	**0.613**	**58.64%**	**41.36%**	
4	4b	**20**	1.326	1.325	1.329	**1.326**	**10.53%**	**89.47%**	
		40	1.197	1.195	1.199	**1.197**	**19.23%**	**80.77%**	
		60	1.015	1.012	1.017	**1.014**	**31.58%**	**68.42%**	**57**
		80	0.959	0.955	0.958	**0.957**	**35.43%**	**64.57%**	
		100	0.820	0.823	0.818	**0.820**	**44.67%**	**55.33%**	
5	4c	**20**	1.292	1.295	1.290	**1.292**	**12.82%**	**87.18%**	
		40	1.108	1.105	1.111	**1.108**	**25.24%**	**74.76%**	
		60	0.981	0.985	0.983	**0.983**	**33.67%**	**66.33%**	
		80	0.837	0.835	0.833	**0.835**	**43.66%**	**56.34%**	**58.79**
		100	0.721	0.725	0.723	**0.723**	**51.21%**	**48.79%**	

3.9 Molecular docking Studies

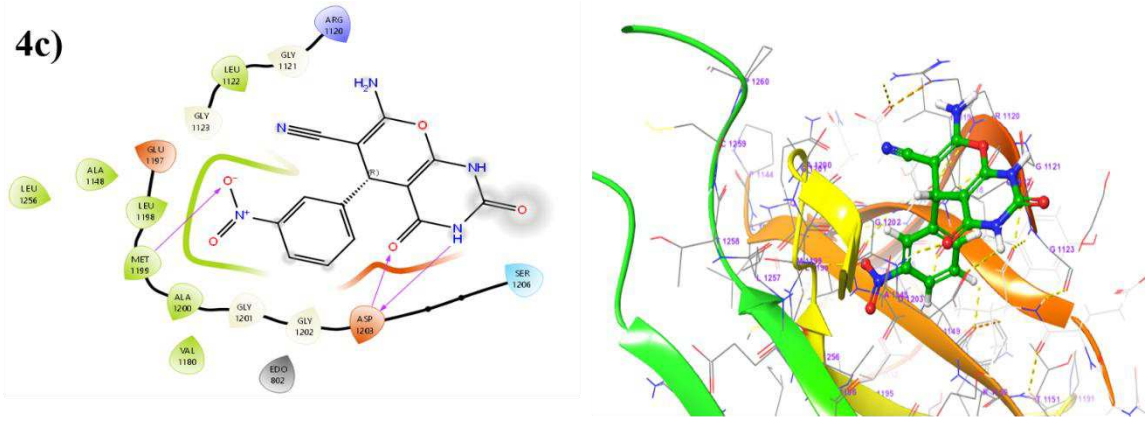
Human Anaplastic Lymphoma Kinase (ALK) is an important receptor kinase which has key role in the brain development but irregulation of it may results in to cancers like non-small cell lung cancer (NSCLC), ALK-positive large cell lymphoma, and neuroblastoma. Human anaplastic lymphoma kinase (ALK) is promising target for development of anticancer agents. Molecular docking of the synthesised derivatives against human anaplastic lymphoma kinase (ALK) indicated good binding affinity. Derivative 4a was found to be interacting via formation of hydrogen bond with MET1119 and ALA1200. Derivative 4b was found to be interacting via formation of hydrogen bond with GLY1201 and GLU1210. Derivative 4c was found to be interacting *via* formation of hydrogen bond with MET1199 and ASP1203. Ligand-protein 2D and 3D interactions are shown in Figure 11.



Docking interaction of derivative 4a: 2D and 3D images



Docking interaction of derivative 4b: 2D and 3D images



Docking interaction of derivative 4c: 2D and 3D images

Fig.11. Binding interactions of compound 4a, 4b and 4c against human anaplastic lymphoma kinase (ALK)

Conclusion

This study emphasizes the viability of eggshell waste as an economical and sustainable resource for the development of a reusable CaO@g-C_3N_4 catalyst, which efficiently facilitates the synthesis of pyrano[2,3-d]pyrimidine scaffolds. The catalyst showed that it may be used several times without losing much of its catalytic power. Structural studies showed that the synthesized CaO@g-C_3N_4 was quite pure. The pyrano[2,3-d]pyrimidines molecules made this way have a lot of potential as cancer treatments, which shows how important this eco-friendly process is. These results show that the catalyst can be used again and again and is stable, which shows that it could be used in solvent-free synthesis in a way that is both cost-effective and environmentally friendly. Overall, this work offers a viable approach to repurposing waste materials, thereby advancing environmentally friendly and cost-effective pharmaceutical synthesis. The synthesized Pyrano[2,3-d]pyrimidine 4a-c derivatives shows good in vitro anticancer activity against SH-SY5Y neuroblastoma cell line. Molecular docking studies against human anaplastic lymphoma kinase (ALK) indicate strong binding affinity.

Supporting Information Summary

The supporting information includes the EDX, ^{1}H NMR, ^{13}C NMR, and LC-MS spectra of selected representative compounds.

Funding The authors received no financial support for the research.

Ethical Approval Not applicable.

Declaration of Conflict of Interest

The authors confirm that there are no known financial interests or personal relationships that could have influenced the work submitted.

Acknowledgment

The authors Sachin Khade sincerely acknowledge Research Fellowship provided by the Chhatrapati Shahu Maharaj Research, Training and Human Development Institute (SARTHI), Pune, under the ‘Research Scheme CSMNRF-2023’.

References

[1] N.S. Naik, S, Divakar M.S. Jyothi, S. Budagumpi, R.G. Balakrishna, M. Padaki, Biogenic-derived eggshell and its derivatives as solid-base heterogeneous catalysts for organic transformations: a comprehensive review. RSC Sustain. 2, 1246–1268 (2024)

[2] M. Baláž, E.V. Boldyreva, D. Rybin, S. Pavlović, D. Rodríguez-Padrón, T. R. Mudrinić, Luque, State-of-the-art of eggshell waste in materials science: recent advances in catalysis, pharmaceutical applications, and mechanochemistry. Front Bioeng. Biotechnol. 8, 612567 (2021)

[3] E. Mosaddegh, A. Hassankhani, Preparation and characterization of nano-CaO based on eggshell waste: a novel and green catalytic approach to highly efficient synthesis of pyrano[4,3-b]pyrans. Chin. J Catal. 35, 351–356 (2014)

[4] O. Awogbemi, F. Inambao, E.I. Onuh, Modification and characterization of chicken eggshell for possible catalytic applications. Heliyon 6, e05283 (2020)

[5] M. Saleem, F. Jamil, O.A. Qamar, P. Akhter, M. Hussain, M.S. Khurram, A.H. Al-Muhtaseb, A. Inayat N.S. Shah, Enhancing the catalytic activity of eggshell-derived CaO catalyst and its application in biodiesel production from waste chicken fat. Catalysts, 12, 1627 (2022)

[6] M. Waheed, M. Yousaf, A. Shehzad, M. Inam-Ur-Raheem, MKI. Khan, M.R. Khan, R.M. Aadil, Channelling eggshell waste to valuable and utilizable products: a comprehensive review. Trends Food Sci. Technol. 106, 78–90 (2020)

[7] M. Lee, W.S. Tsai, S.T. Chen, Reusing shell waste as a soil conditioner alternative? A comparative study of eggshell and oyster shell using a life cycle assessment approach. J Clean Prod. 265, 121845 (2020)

[8] A.Y. El-Khateeb, S.E. Hamed, K.M. Elattar, Recent advancements in the multicomponent synthesis of heterocycles integrated with a pyrano[2,3-d]pyrimidine core. RSC Adv. 12, 11808–11842 (2022)

[9] N.R. Kamdar, D.D. Haveliwala, P.T. Mistry, S.K. Patel, Design, synthesis and in vitro evaluation of antitubercular and antimicrobial activity of some ovel pyranopyrimidines. Eur. J Med. Chem. 45, 5056–5063 (2010)

[10] Abd El-Sattar NEA, Badawy EHK, Elrazaz EZ, Ismail NSM. Discovery of pyrano[2,3-d]pyrimidine-2,4-dione derivatives as novel PARP-1 inhibitors: design, synthesis and antitumor activity. RSC Adv. 11, 1–12 (2021)

[11] MHM. AbdEl-Azim, M.A. Aziz, S.M. Mouneir, A.F. El-Farargy, W.S. Shehab. Ecofriendly synthesis of pyrano[2,3-d]pyrimidine derivatives and related heterocycles with anti-inflammatory activities. Arch Pharm. 353, 2000084 (2020)

[12] S. Poola, M.S. Shaik, M. Sudileti, S. Yakkate, V. Nalluri, A. Chippada, S.R. Cirandur, Nano CuO–Ag-catalyzed synthesis of some novel pyrano[2,3-d]pyrimidine derivatives and evaluation of their bioactivity. J Chin. Chem. Soc. 67, 805–820 (2020)

[13] N.E. Abd El-Sattar, K. El-Adl, M.A. El-Hashash, S.A. Salama, M.M. Elhady, Design, Synthesis, molecular docking, and in silico ADMET profile of pyrano[2,3-d]pyrimidine derivatives as antimicrobial and anticancer agents. Bioorg. Chem. 115, 105186 (2021)

[14] N.D. Thanh, NTK. Giang, N.T.T. Ha, D.T. Tung, C.T. Le, H.T.K. Van, V.N. Toan, Synthesis and in vitro anticancer activity of 4H-pyrano[2,3-d]pyrimidine–1H-1,2,3-triazole hybrid compounds bearing a D-glucose moiety with dual EGFR/HER2 inhibitory activity and induced-fit docking study. J. Mol. Struct. 1271, 133932 (2023)

[15] RMR. Sirigireddy, S. Shaik, M. Gundluru, S.R. Cirandur, F. Alonso-Marroquin, R.R. Kakarla, T.M. Aminabhavi, Fused chromeno-pyrano-pyrimidinediones: multicomponent green synthesis and electrochemical properties. J Mol. Liq. 396, 123950 (2024)

[16] D.S. Hai, N.T.T. Ha, D.T. Tung, C.T. Le, H.H. Anh, V.N. Toan, N.D. Thanh, N-propargylation reaction of substituted 4H-pyrano[2,3-d]pyrimidine derivatives under conventional, ultrasound-, and microwave-assisted conditions. Chem. Pap. 76, 5281–5292 (2022)

[17] A. Khazaei, H.A.A. Nik, A.R. Moosavi-Zare, Water-mediated domino Knoevenagel–Michael–cyclocondensation reaction of malononitrile, various aldehydes, and barbituric acid derivatives using boric acid aqueous solution system compared with nano-titania sulfuric acid, J. Chin. Chem. Soc 62,

675–679 (2015)

[18] R. Vaid, N. Sharma, M. Gupta, B. Chowhan. Nanosized calcined mixed oxides-supported alkali metal (K_2O/Al_2O_3–CaO) as solid base catalyst: preparation and investigation of its catalytic efficiency in the synthesis of benzylidene malononitriles/barbiturates and in pyrano[2,3-d]pyrimidines, J. Iran. Chem. Soc. 19, 2855–2870 (2022)

[19] S. Azad Poshtmakhi, K. Rad-Moghadam, H. Hosseinzadeh, S. Toorchi-Roudsari, Finely dispersed Fe_3O_4 and Ag nanoparticles adhered by starch nanolayers: an efficient catalyst for the synthesis of pyrano[2,3-d]pyrimidines, ChemistrySelect 8, e202300533 (2023)

[20] M.M. Heravi, A. Ghods, K. Bakhtiari, F. Derikvand, Zn[(L)-proline]$_2$: an efficient catalyst for the synthesis of biologically active pyrano[2,3-d]pyrimidine derivatives, Synth. Commun. 40, 1927–1931 (2010)

[21] F. Mohamadpour, Green synthesis of pyrano[2,3-d]pyrimidine scaffolds in cetyltrimethylammonium bromide (CTAB) micellar media. Curr. Res. Green Sustain. Chem. 10, 100456 (2025).

[22] A.R. Bhat, A.H. Shalla, R.S. Dongre, Dibutylamine (DBA): a highly efficient catalyst for the synthesis of pyrano[2,3-d]pyrimidine derivatives in aqueous media, J Taibah Univ. Sci. 10, 9–18 (2016)

[23] G.M. Ziarani, S. Faramarzi, S. Asadi, A. Badiei, R. Bazl, M. Amanlou, Three-component synthesis of pyrano[2,3-d]pyrimidine-2,4-dione derivatives facilitated by sulfonic acid nanoporous silica (SBA-Pr-SO_3H) and their docking and urease inhibitory activity, DARU J Pharm. Sci. 21, 3 (2013).

[24] Jolodar OG, Shirini F, Seddighi M. Efficient synthesis of pyrano[2,3-d]pyrimidinone and pyrido[2,3-d]pyrimidine derivatives in the presence of a novel basic ionic liquid catalyst, Chin. J Catal. 38, 1245–1251 (2017)

[25] A. Jahanbakhshi, M. A. Farahi, Novel magnetic FSM-16-supported ionic liquid/Pd complex as a high-performance and recyclable catalyst for the synthesis of pyrano[3,2-c]chromenes, RSC Adv. 14, 16401-16410 (2024)

[26] M.H. Sayahi, Ionic liquid-modified SPION@chitosan as an efficient catalyst for multicomponent condensations, Catalysts, 13, 290 (2023)

[27] T. Farahmand, S. Hashemian, A. Sheibani, One-pot synthesis of pyrano[2,3-d]pyrimidinones using Mn-ZIF-8@$ZnTiO_3$ nanocatalyst, J. Mol. Struct. 1206, 127667 (2020)

[28] R. Keshani, N. Hazeri, H. Faroughi Niya, M. Fatahpour, Synthesis of benzo[b]pyran and pyrano[2,3-d]pyrimidine derivatives using a new superparamagnetic nanocatalyst Fe_3O_4@gly@furfural@$Co(NO_3)_2$, Res. Chem. Intermed. 49, 3461–3479 (2023)

[29] M.P. Parmar, R.M. Vala, H.M. Patel, Importance of hybrid catalysts toward the synthesis of 5H-pyrano [2,3-d]pyrimidinones/2,4-diones, ACS Omega, 8, 1759–1816 (2023)

[30] S. Sreekantan, A.K. Sudhakaran, B. Marimuthu, Upcycling solid wastes: using abundant eggshell wastes for the greener production of lactic acid under ambient conditions, J Environ. Chem. Eng. 13, 115603 (2025)

[31] H. Zhaleh, H. Mehdizadeh, S. Khoshkhoy, Punica granatum seed essential oil suppressed methadone-induced cell death by natural antioxidant activity, Asian Pac. J. Cancer Prev. 24, 801 (2023)

[32] RCSB PDB (RCSB.org), US data center for the global Protein Data Bank (PDB)

[33] H. Sakamoto, T. Tsukaguchi, S. Hiroshima, T. Kodama, T. Kobayashi, T.A. Fukami, Y. Aoki,

CH5424802, a selective ALK inhibitor capable of blocking the resistant gatekeeper mutant, Cancer Cell 19, 679–690 (2011)

[34] E.F. Pettersen, T.D. Goddard, C.C. Huang, G.S. Couch, D.M. Greenblatt, E.C. Meng, T.E. Ferrin, UCSF Chimera visualization system for exploratory research and analysis, J. Comput. Chem. 25, 1605–1612 (2004)

[35] B. Baba, Ç.Z. Köprü, I. Yildiz, E. Yardimci, A. Akbay, Anticancer activity and molecular docking analysis of selected benzoxazole derivatives as apoptosis inducers in non-small cell lung cancer, J Clin. Pract. Res. 48, 42 (2026)

[36] A. Roy, S.S. Gauri, M. Bhattacharya, J. Bhattacharya, Antimicrobial activity of CaO nanoparticles, J Biomed. Nanotechnol. 9, 1570–1578 (2013)

[37] R.G. Jalu, T.A. Chamada, R. Kasirajan, Calcium oxide nanoparticles synthesized from hen eggshells for the removal of Pb(II) from aqueous solution, Environ. Challenges 4, 100193 (2021)

[38] R.B. Said, S. Rahali, M.A. Ben Aissa, A. Albadri, A. Modwi, Uptake of BF dye from the aqueous phase by CaO-g-C_3N_4 nanosorbent: construction, description, and recyclability, Inorganics, 11, 44 (2023)

[39] A. Maleki, M. Niksefat, J. Rahimi, R. Taheri-Ledari, Multicomponent synthesis of pyrano[2,3-d]pyrimidine derivatives via a direct one-pot strategy executed by novel designed copperated Fe_3O_4@polyvinyl alcohol magnetic nanoparticles, Mater Today Chem, 13, 110–120 (2019)

[40] S. Momeni, R. Ghorbani-Vaghei, Copper immobilized on modified LDHs as a novel efficient catalytic system for three-component synthesis of pyrano[2,3-d]pyrimidine and pyrazolo[4′,3′:5,6]pyrano[2,3-d]pyrimidine derivatives, ACS Omega 9, 10332–10342 (2024)

[41] O.A.A. Alabrahim, A.M. Abdeldayem, H.M.E.S. Azzazy. Enhanced cytotoxic activity of Moringa oleifera–loaded pharmacosomes against neuroblastoma. Nanoscale Adv. (2026).

[42] A. Rosa, F. Pollastro, V. Sogos, F. Piras, Comparative evaluation of cytotoxic and apoptotic effects of natural compounds in SH-SY5Y neuroblastoma cells in relation to their physicochemical properties. Molecules, 30, 1742 (2025)

[43] R.G. Mahardika, A. Danova, C. Aonbangkhen, J. Chatwichien, S. Wongsuwan, W. Chavasiri, A. Alni, Unraveling the anticancer activity of suitinib derivatives through modifications in solvent-exposed regions: synthesis, in vitro evaluation, and computational studies, Arch. Pharm, 358, e70168 (2025)

[44] M.B. Hansen, S.E. Nielsen, K. Berg, Re-examination and further development of a precise and rapid dye method for measuring cell growth/cell kill, J Immunol. Methods, 119, 203–210 (1989)

[45] M.M. Ribeiro, L.S. Lima, N.D.S. da Costa, M.E. Pereira, A.S. Fonseca, L.R. Cavalli, C.S. Oliveira, In vitro effects of retinoic acid and sodium selenite on neuroblastoma cell line (SH-SY5Y), Future Pharmacol, 5, 65 (2025)

Supplementary Files

This is a list of supplementary files associated with this preprint. Click to download.

- SupportingInformationCaO.docx